J|A|C|S
ARTICLES
Published on Web 12/16/2005

Influence of Intermolecular Orientation on the Photoinduced Charge Transfer Kinetics in Self-Assembled Aggregates of Donor−Acceptor Arrays

Edwin H. A. Beckers,[†] Stefan C. J. Meskers,[†] Albertus P. H. J. Schenning,[†] Zhijian Chen,[‡] Frank Würthner,[‡] Philippe Marsal,[§] David Beljonne,[§] Jérôme Cornil,[§] and René A. J. Janssen*[,†]

Contribution from the Laboratory of Macromolecular and Organic Chemistry, Eindhoven University of Technology, P.O. Box 513, NL-5600 MB Eindhoven, The Netherlands, Institut für Organische Chemie, Universität Würzburg, Am Hubland, D-97074 Würzburg, Germany, and Laboratory for Chemistry of Novel Materials, University of Mons-Hainaut, Place du Parc 20, B-7000 Mons, Belgium

Received October 5, 2005; E-mail: r.a.j.janssen@tue.nl

Abstract: The kinetics of photoinduced charge transfer reactions in covalently linked donor−acceptor molecules often undergoes dramatic changes when these molecules self-assemble from a molecular dissolved state into a nanoaggregate. Frequently, the origin of these changes is only partially understood. In this paper, we describe the intermolecular spatial organization of three homologous arrays, consisting of a central perylene bisimide (PERY) acceptor moiety and two oligo(*p*-phenylene vinylene) (OPV) donor units, in nanoaggregates and identify both face-to-face (H-type) and slipped (J-type) stacking of the OPV and PERY chromophores. For the J-type aggregates, short intermolecular OPV−PERY distances are created that give rise to a charge-transfer absorption band. The proximity of the donor and acceptor groups in the J-type aggregates enables a highly efficient photoinduced charge separation with a rate ($k_{cs} > 10^{12}$ s^{-1}) that significantly exceeds the rate of the intramolecular charge transfer of the same compounds when molecularly dissolved, even in the most polar media. In the H-type aggregates, on the other hand, the intermolecular OPV−PERY distance is not reduced compared to the intramolecular separation, and hence, the rates of the electron transfer reactions are not significantly affected compared to the molecular dissolved state. Similar to the forward electron transfer, the kinetics of the charge recombination in the aggregated state can be understood by considering the different interchromophoric distances that occur in the H- and J-type aggregates. These results provide the first consistent rationalization of the remarkable differences that are observed for photoinduced charge-transfer reactions of donor−acceptor compounds in molecularly dissolved versus aggregated states.

Introduction

Photoinduced charge-transfer in donor−acceptor molecules is fairly well understood, in particular for covalently linked diads in solution.[1,2] In molecular diads, triads, tetrads, and more extended arrays containing different photoactive and redox-active chromophores, photoinduced charge separation can result in long-lived charge-separated states. Various carefully designed energy- and electron-transfer cascades that mimic the steps occurring in natural photosynthesis have been synthesized and investigated in great detail.[3,4] In general, the energetics and kinetics of the formation of these charge-separated states can be adequately described by theories of Marcus and Jortner when taking into account the orientation, distance, and nature of the linker between the donor and acceptor chromophores.[5,6]

In contrast, characterization and insight into photoinduced electron transfer in self-assembled nanoscale (10−100 nm) architectures is only at its beginning. Of course it is well established that chlorophylls work in concert in photosynthesis to funnel light energy to the reaction center prior to a cascade of electron-transfer reactions. However, the collective behavior of chromophores related to photoinduced electron transfer has not received much attention in artificial systems. We are interested in studying photoinduced charge transfer and recombination in donor−acceptor molecules that are able to self-organize into nanoaggregates or stacks in solution, either by lowering the temperature or by changing the polarity of the solvent. The self-assembly enables the controlled growth of nanoaggregates and provides a unique approach to gain insight

[†] Eindhoven University of Technology.
[‡] Universität Würzburg.
[§] University of Mons-Hainaut.

(1) *Advances in Chemical Physics*; Jortner, J., Bixon, M., Ed.; Wiley-Interscience: New York, 1999; Vols. 106 and 107.
(2) *Electron Transfer in Chemistry*; Balzani, V., Ed.; Wiley-VCH: Weinheim, 2001; Vols. 1−5
(3) Gust, D.; Moore, T. A.; Moore, A. L. *Acc. Chem. Res.* **1993**, *26*, 198−205.
(4) Gust, D.; Moore, T. A.; Moore, A. L. *Acc. Chem. Res.* **2001**, *34*, 40−48.
(5) Paddon-Row, M. N. *Acc. Chem. Res.* **1994**, *27*, 18−25.
(6) Guldi, D. M. *Chem. Soc. Rev.* **2002**, *31*, 22−36.

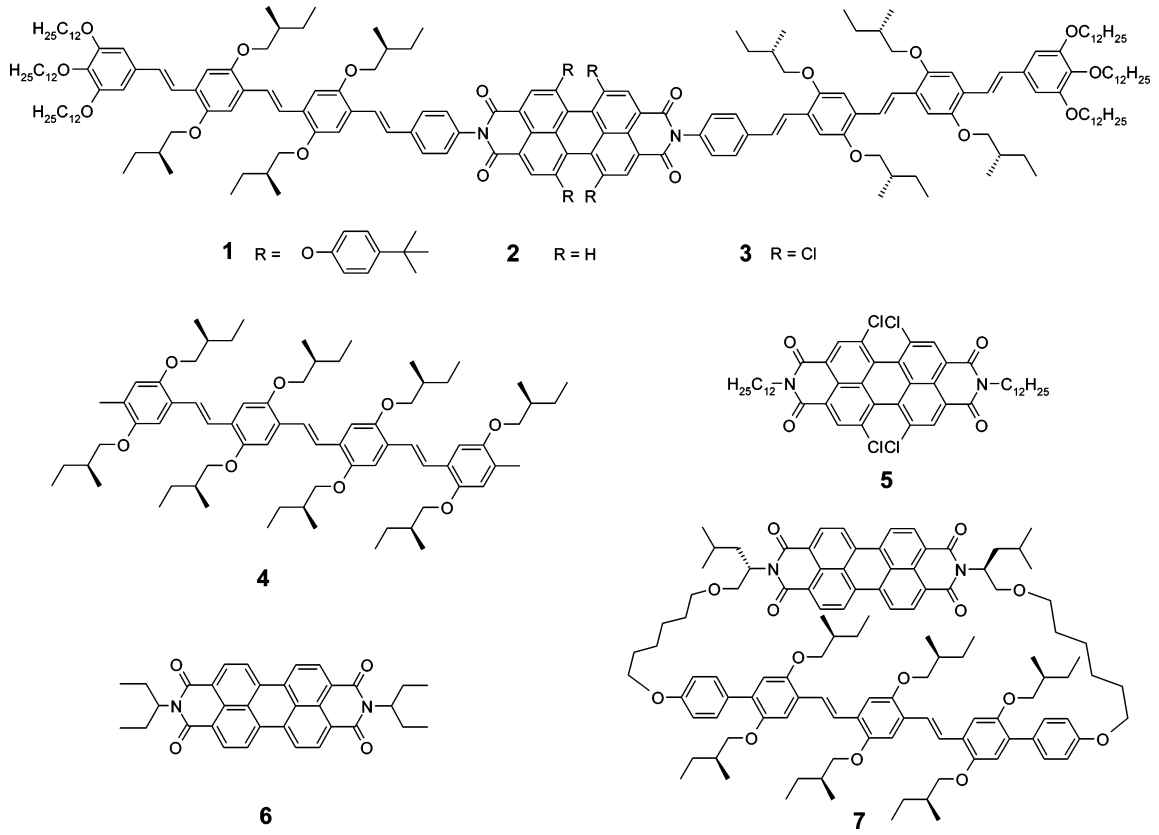

Figure 1. Studied OPV−PERY−OPV arrays **1**−**3** together with the OPV (**4**) and perylene bisimide (**5**, **6**) reference compounds and the cyclic OPV−PERY dimer **7**.

in the transition in photophysical properties when single diad molecules are transformed into a material. Ultimately, these insights may provide new routes toward charge separation, energy conversion, and storage assemblies.

Various recent results indicate that the photophysics of nanoassemblies, in which multiple covalently linked donor and acceptor systems are interacting with each other, can be dramatically different when compared to those of isolated compounds; however, the reasons for these differences are not always well understood. Wasielewski et al. reported ordered nanoparticles of tetrakis(perylene bisimide)porphyrins in which donors and acceptors are stacked.[7] The forward electron transfer in these photofunctional nanoparticles is faster and the recombination slower compared to model compounds that do not form these aggregates under similar conditions. In this system, the stabilization of the charge-separated state occurs via migration of charges between closely coupled redox-active groups. In another example, we observed that the forward electron transfer in oligo(phenylene vinylene)−fullerene diads can be up to an order of magnitude faster in thin films than the same reaction in the most polar solvents.[8] Taking into account that organic solids have a much lower relative dielectric constant (typically $\epsilon_r = 3$ to 4) compared to the most polar solvents used ($\epsilon_r = 25$), the increased transfer speed cannot be explained by the polarity. A similar order of magnitude increase was found in fine particles of oligothiophene−fullerene diads when compared to benzonitrile solution.[9] For perylene bisimide systems, rate constants for charge separation exceeding 10^{12} s^{-1} have been observed in aggregated structures, where the formation of a charge separated state is not energetically favorable in the molecularly dissolved state.[10−12] Each of these examples demonstrates that aggregate formation leads to unexpected kinetics for photoinduced charge separation.

It is our goal to rationalize some of the dramatic changes that occur in the photophysics of covalently linked donor−acceptor molecules upon aggregation. Herein, we correlate the intermolecular distance between the donor and acceptor chromophores in self-assembled aggregates with the kinetics of the photoinduced charge separation and recombination reactions. By using covalently linked donor−acceptor model systems, we can directly differentiate between intramolecular and intermolecular effects by comparing molecular dissolved and aggregated solutions, respectively. In this study, we use three related oligo(*p*-phenylene vinylene) (OPV)−perylene bisimide (PERY) arrays (Figure 1). These arrays were considered as an appropriate starting point for this study because the photoinduced charge transfer between these chromophores in solution has been extensively studied,[13−17] and the individual chromophores are

(7) Van der Boom, T.; Hayes, R. T.; Zhao, Y.; Bushard, P. J.; Weiss, E. A.; Wasielewski, M. R. *J. Am. Chem. Soc.* **2002**, *124*, 9582−9590.
(8) Van Hal, P. A.; Meskers, S. C. J.; Janssen, R. A. J. *Appl. Phys. A* **2004**, *79*, 41−46.
(9) Fujitsuka, M.; Masuhara, A.; Kasai, H.; Oikawa, H.; Nakanishi, H.; Ito, O.; Yamashiro, T.; Aso, Y.; Otsubo, T. *J. Phys. Chem. B* **2001**, *105*, 9930−9934.
(10) Fuller, M. J.; Sinks, L. E.; Rybtchinski, B.; Giaimo, J. M.; Li, X.; Wasielewski, M. R. *J. Phys. Chem. A* **2005**, *109*, 970−975.
(11) Rybtchinski, B.; Sinks, L. E.; Wasielewski, M. R. *J. Am. Chem. Soc.* **2004**, *126*, 12268−12269.
(12) Würthner, F.; Chen, Z.; Hoeben, F. J. M.; Osswald, P.; You, C.-C.; Jonkheijm, P.; van Herrikhuyzen, J.; Schenning, A. P. H. J.; van der Schoot, P. P. A. M.; Meijer, E. W.; Beckers, E. H. A.; Meskers, S. C. J.; Janssen, R. A. J. *J. Am. Chem. Soc.* **2004**, *126*, 10611−10618.

known to form supramolecular aggregates in a variety of apolar solvents.[12,18,19] Previous studies on aggregates containing OPV[20,21] or PERY[7,22,23] moieties have revealed that stacking provides the possibility for excitations to hop to different sites within the same supramolecular structure or to delocalize over several chromophores.

The three homologous OPV−PERY−OPV arrays used in this study consist of the same donor and acceptor building blocks, the only difference being the four substituents on the bay position of the perylene bisimide moiety. For compound **1**,[12] these are *tert*-butylphenoxy substituents, whereas for compounds **2**[13] and **3**[15] the substituents are respectively hydrogen and chlorine. The different substituents influence the acceptor part of the system.[15] Moreover, the planarity of the perylene bisimide changes with the bay substituents. An almost flat conformation is expected for the hydrogen-substituted perylene bisimide moiety, while torsion angles of 25° and 37° have been observed for phenoxy- and chlorine-substituted perylene bisimides as a result of the increased steric hindrance.[24−27] This twisting is expected to affect the packing of the compounds in aggregates, while the differences in acceptor strength influence intermolecular donor−acceptor interactions.

The insights into the supramolecular organization, as inferred from optical absorption spectra and molecular mechanics calculations, provide a consistent description of the remarkable differences between the picosecond charge-transfer kinetics in OPV−PERY−OPV arrays in molecularly dissolved versus aggregated states when the distance between chromophores is the essential parameter.

Results and Discussion

Intermolecular Organization in the Aggregates from Absorption Spectroscopy. To understand the differences in photophysics between isolated molecules and molecules in nanoaggregates or thin films, knowledge and control over the mesoscopic ordering of the molecules are crucial but, in general, difficult to obtain.[4,26,28−30] Typically π-conjugated oligomers assemble in small aggregates or stacks with lateral dimensions of several nanometers and lengths up to micrometers.[31−34] Although in favorable cases, techniques such as X-ray diffraction (XRD), small angle neutron scattering (SANS), transmission electron microscopy (TEM), or atomic force microscopy (AFM) can be used to determine the dimensions and supramolecular structure of aggregates,[7,31−34] we found this cumbersome for the present compounds. We noticed that, among others, the concentration, surface interaction, temperature, and processing conditions often have an extremely large influence on the structures obtained. To enable a direct comparison of the structural information and the photophysics, we decided that both should preferably be studied under identical conditions, and we therefore focused our attention on the detailed analysis of the absorption spectra of the aggregated OPV−PERY−OPV arrays as dilute solutions in methylcyclohexane (MCH).

The UV−vis absorption spectra of the arrays **1**−**3** in MCH are characterized by a strong band of the OPV units centered at ∼425 nm and one or more vibronic transitions of the PERY core at higher wavelengths. The distinct changes that can be observed in the spectra recorded at 20 and 90 °C are consistent with the presence of aggregates at low temperature (Figure 2). Upon heating a solution of **1** in MCH from 20 to 90 °C, a shift of the perylene bisimide maximum from 580 to 565 nm is observed. This shift is typical of the dissociation of the supramolecular structure as a result of the increased temperature.[12] On the basis of the red shift of the perylene bisimide absorption maximum of **1** upon aggregation, it is here proposed that a J-type aggregate (Figure 3) is obtained.[35,36] The OPV absorption shows a small (424−432 nm) red shift in the same temperature range. In principle, the change in refractive index of the solvent with temperature can contribute to the observed shift.[37] We find, however, that the observed shift is larger than expected from the change in refractive index. More importantly, in a previous study[12] we have shown that the spectral changes can also be induced by changing the concentration at constant temperature. This shows that the spectral changes are mainly due to aggregation.

For **3** similar red shifts are observed; the perylene bisimide absorption maximum shifts from 513 nm for molecularly dissolved species at elevated temperature to 528 nm for the aggregated species at room temperature, while the OPV unit shifts from 428 to 446 nm. This implies that for **3** a J-type structure may also exist. For **2**, the changes in the spectra seem slightly more complex. Compared to the sharp perylene bisimide vibronic at 515 nm, a new (weak) band appears at ∼550 nm upon aggregation, while at the same time the intensity at ∼470

(13) Peeters, E.; Van Hal, P. A.; Meskers, S. C. J.; Janssen, R. A. J.; Meijer, E. W. *Chem.-Eur. J.* **2002**, *8*, 4470−4474.
(14) Neuteboom, E. E.; Meskers, S. C. J.; Van Hal, P. A.; van Duren, J. K. J.; Meijer, E. W.; Janssen, R. A. J.; Dupin, H.; Pourtois, G.; Cornil, J.; Lazzaroni, R.; Brédas, J.-L.; Beljonne, D. *J. Am. Chem. Soc.* **2003**, *125*, 8625−8638.
(15) Beckers, E. H. A.; Meskers, S. C. J.; Schenning, A. P. H. J.; Chen, Z.; Würthner, F.; Janssen, R. A. J. *J. Phys. Chem. A* **2004**, *108*, 6933−6937.
(16) Ramos, A. M.; Beckers, E. H. A.; Offermans, T.; Meskers, S. C. J.; Janssen, R. A. J. *J. Phys. Chem. A* **2004**, *108*, 8201−8211.
(17) Ramos, A. M.; Meskers, S. C. J.; Beckers, E. H. A.; Prince, R. B.; Brunsveld, L.; Janssen, R. A. J. *J. Am. Chem. Soc.* **2004**, *126*, 9630−9644.
(18) Schenning, A. P. H. J.; van Herrikhuyzen, J.; Jonkheijm, P.; Chen, Z.; Würthner, F.; Meijer, E. W. *J. Am. Chem. Soc.* **2002**, *124*, 10252−10253.
(19) Neuteboom, E. E.; Van Hal, P. A.; Janssen, R. A. J. *Chem.-Eur. J.* **2004**, *10*, 3907−3918.
(20) Herz, L. M.; Daniel, C.; Silva, C.; Hoeben, F. J. M.; Schenning, A. P. H. J.; Meijer, E. W.; Friend, R. H.; Phillips, R. T. *Phys. Rev. B* **2003**, *68*, 045203/1−045203/7.
(21) Hoeben, F. J. M.; Herz, L. M.; Daniel, C.; Jonkheijm, P.; Schenning, A. P. H. J.; Silva, C.; Meskers, S. C. J.; Beljonne, D.; Phillips, R. T.; Friend, R. H.; Meijer, E. W. *Angew. Chem., Int. Ed.* **2004**, *43*, 1976−1979.
(22) Herz, L. M.; Silva, C.; Friend, R. H.; Phillips, R. T.; Setayesh, S.; Becker, S.; Marsitsky, D.; Müllen, K. *Phys Rev. B* **2001**, *64*, 195203/1−195203/9.
(23) Li, X.; Sinks, L. E.; Rybtchinski, B.; Wasielewski, M. R. *J. Am. Chem. Soc.* **2004**, *126*, 10810−10811.
(24) Würthner, F.; Sautter, A.; Thalacker, C. *Angew. Chem., Int. Ed.* **2000**, *39*, 1243−1245.
(25) Hofkens, J.; Vosch, T.; Maus, M.; Kohn, F.; Cotlet, M.; Weil, T.; Herrmann, A.; Müllen, K.; De Schryver, F. C. *Chem. Phys. Lett.* **2001**, *333*, 255−263.
(26) Chen, Z.; Debije, M. G.; Debaerdemaeker, T.; Osswald, P.; Würthner, F. *ChemPhysChem* **2004**, *5*, 137−140.
(27) Leroy-Lhez, S.; Baffreau, J.; Perrin, L.; Levillain, E.; Allain, M.; Blesa, M.-J.; Hudhomme, P. *J. Org. Chem.* **2005**, *70*, 6313−6320.
(28) Tributsch, H.; Pohlmann, L. *Science* **1998**, *279*, 1891−1895.
(29) Struijk, C. W.; Sieval, A. B.; Dakhorst, J. E. J.; van Dijk, M.; Kimkes, P.; Koehorst, R. B. M.; Donker, H.; Schaafsma, T. J.; Picken, S. J.; van de Craats, A. M.; Warman, J. M.; Zuilhof, H.; Sudhölter, E. J. R. *J. Am. Chem. Soc.* **2000**, *122*, 11057−11066.
(30) Schmidt-Mende, L.; Fechtenkotter, A.; Müllen, K.; Moons, E.; Friend, R. H.; MacKenzie, J. D. *Science* **2001**, *293*, 1119−1122.
(31) Hudson, S. D.; Jung, H. T.; Percec, V.; Cho, W. D.; Johansson, G.; Ungar, G.; Balagurusamy, V. S. K. *Science* **1997**, *278*, 449−452.
(32) Apperloo, J. J.; Janssen, R. A. J.; Malenfant, P. R. L.; Fréchet, J. M. J. *J. Am. Chem. Soc.* **2001**, *125*, 6916−6924.
(33) Percec, V.; Glodde, M.; Bera, T. K.; Miura, Y.; Shiyanovskaya, I.; Singer, K. D.; Balagurusamy, V. S. K.; Heiney, P. A.; Schnell, I.; Rapp, A.; Spiess, H. W.; Hudson, S. D.; Duan, H. *Nature* **2002**, *419*, 384−387.
(34) Hoeben, F. J. M.; Jonkheijm, P.; Meijer, E. W.; Schenning, A. P. H. J. *Chem. Rev.* **2005**, *105*, 1491−1546.
(35) Kasha, M. *Rad. Res.* **1963**, *20*, 55−70.
(36) Würthner, F.; Thalacker, C.; Diele, S.; Tschierske, C. *Chem. Eur. J.* **2001**, *7*, 2245−2253.
(37) Weigang, O. E. *J. Chem. Phys.* **1960**, *33*, 892−899.

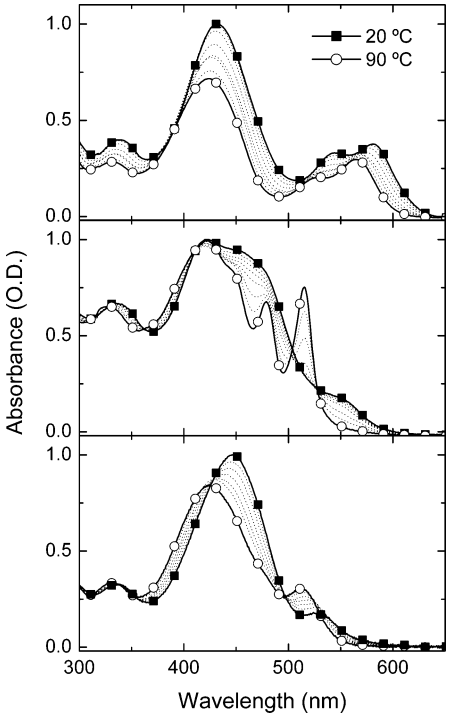

Figure 2. Absorption spectra of **1** (top, 5×10^{-5} M), **2** (middle, 2×10^{-6} M), and **3** (bottom, 1.3×10^{-6} M) measured in MCH. The solid squares show the absorption spectra recorded at 20 °C, whereas the open circles indicate the results obtained at 90 °C. The spectra were not corrected for changes in density and refractive index of the solvent with temperature.

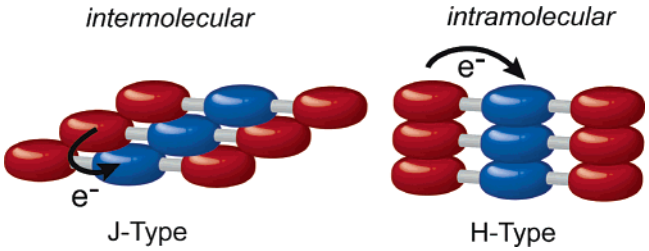

Figure 3. Cartoon of the two limiting situations for the one-dimensional packing of OPV−PERY−OPV arrays to give J-type (left) and H-type (right) aggregates.

nm is increased. Such a blue shift of the absorption maximum and an accompanying low-intensity band at lower energy are typical for the formation of H-type aggregates formed. In agreement with previous observations, the differences in aggregation observed for **1** and **3** versus **2** are consistent with the fact that the expected increased bulkiness and twist induced by the *tert*-butylphenoxy and chlorine substituents for **1** and **3**[24−27,36] hamper a face-to-face packing of these chromophores, as required for H-type aggregation. We note that for all aggregates some degree of rotational displacement may also be present.

A study on the concentration dependence of the aggregation behavior at room temperature indicated that for concentrations above 1×10^{-5} M in MCH all three compounds are only present as aggregated species. For **1** only 50% of the molecules is aggregated in MCH at a concentration of 4×10^{-7} M, whereas this occurs at a concentration of 5×10^{-8} M for **3**. At the lowest concentration where an absorption signal is detectable (1×10^{-8} M), compound **2** is still completely aggregated.

Compounds **1**−**3** bear eight enantiomerically pure (*S*)-2-methylbutoxy substituents. This side chain chirality can result in a circular dichroism of the $\pi-\pi^*$ transitions of the OPV and PERY

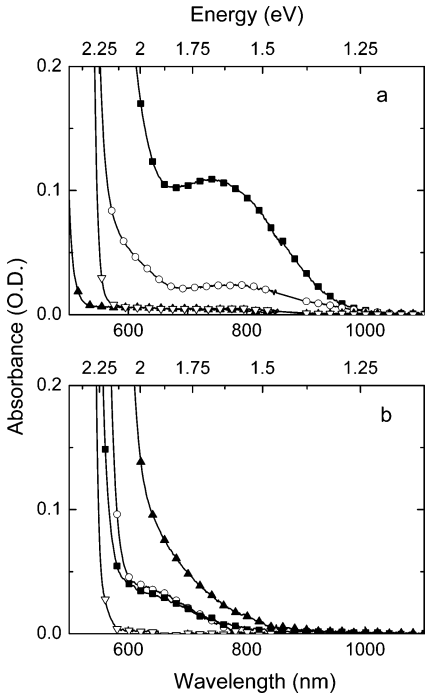

Figure 4. (a) Absorption spectra of **3** (solid squares, 1.3×10^{-4} M), **4** (solid triangles, 10^{-4} M), **5** (open triangles, 10^{-4} M), and a 1:1 mixture of **4** and **5** (open circles, 10^{-4} M) in MCH at 20 °C. (b) Absorption spectra of **7** in MCH (solid squares, 2×10^{-4} M) and THF (open circles, 2×10^{-4} M), **2** in MCH (solid triangles, 2×10^{-4} M), and a 1:1 mixture of **4** and **6** in THF (open triangles, 2×10^{-4} M).

chromophores when the molecules aggregate in a helical fashion. Small circular dichroism signals, originating from interchromophoric coupling, are indeed observed for **1**−**3** in MCH (see Supporting Information) and disappear upon heating. The CD signal evidences some rotational displacement in the aggregates.

More evidence for the presence of a J-type aggregate structure for **3** in MCH has been obtained by analyzing the absorption spectra at higher concentration (Figure 4a). Under these conditions and at the same concentrations, an absorption band that is not present for the separate reference compounds **4** and **5** can be observed for **3** in the region from 700 to 1000 nm. This band points to the occurrence of charge transfer (CT) between the two *different* chromophores in the ground state. In addition, the onset of the PERY($S_1 \leftarrow S_0$) transition has slightly shifted to longer wavelengths as compared to the reference compounds. This shift is due to the dipole-allowed low-energy absorption that is characteristic for transition dipoles in a head-to-tail configuration in a J-type aggregate. The observed CT band is only expected when the OPV and perylene bisimide chromophores are in a face-to-face orientation. Because all molecules are aggregated at the concentrations used, a value of 800 $L \cdot mol^{-1} \cdot cm^{-1}$ can be calculated as a lower limit for the molar absorption coefficient of this transition, based on the assumption that all present molecules will participate in forming such face-to-face aggregates.

Previously, it has been observed that the introduction of chlorine substituents on the bay position increases the tendency of perylene bisimide molecules to form intermolecular charge complexes with other aromatic molecules.[38] Therefore, we also studied a mixture of **4** and **5** in order to see if a face-to-face OPV−PERY complex can be obtained when the OPV and PERY moieties are not covalently linked. As can be seen in

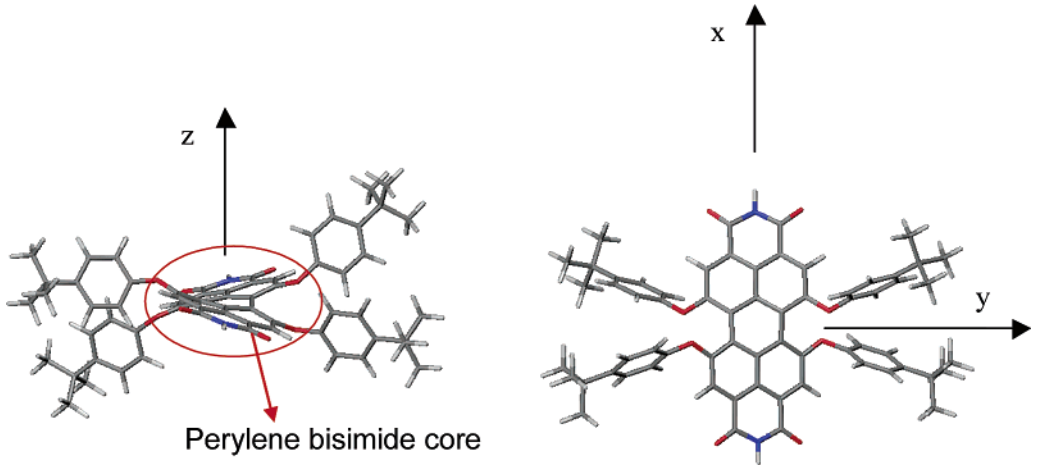

Figure 5. Illustration of the bending of the perylene bisimide core in **1** (left) and of the extended structure used in the MM calculations (right). The stacking axis *z* and the translational axis *x* are also defined.

Figure 4, the 1:1 mixture of **4** and **5** in MCH at 10^{-4} M gives rise to the CT absorption band, demonstrating that the OPV and PERY compounds also have a tendency to stack on top of each other when they are not covalently linked. This implies that the mixed system gains energy by forming a charge-transfer complex in the ground state in which the π-electron systems of both compounds are in a sandwich-type configuration. Although the concentrations used in the experiment are similar for array **3** and the mixture of **4** and **5**, the intensity of the CT absorption band is lower for the mixture, while the spectral positions are the same. This indicates that in the mixture not all molecules are forming a donor−acceptor aggregate; as can be expected, the intensity of the CT band decreases with temperature as a result of a shift in this equilibrium. A semilogarithmic plot of the intensity of the absorption band at 790 nm versus reciprocal temperature provided a binding enthalpy of −110 meV (−10.6 kJ/mol) for the association of the complex containing **4** and **5**.

In addition to the chlorine substituted perylene bisimide compounds, the presence of a charge-transfer absorption in the ground state was also studied for the OPV−PERY array **2**. This is, however, less straightforward because **2** is believed not to form aggregates composed of two *different* chromophores in a face-to-face orientation.[39] By looking at the absorption spectrum it is therefore not surprising that for **2** the only visible difference with respect to the reference compounds **4** and **6** is a slight red shift of the absorption onset, caused by the presence of H-aggregates (Figure 4b). Unfortunately, it proved not possible to study the mixture of **4** and **6** because of the limited solubility of **6** in MCH. Therefore, the cyclic OPV−PERY dimer **7** was used as a model compound. As a result of the strained geometry within **7**, the donor and acceptor moieties are always positioned on top of each other. As a consequence, an extra absorption is observed between 600 and 800 nm in MCH. In addition, this band is also observed in THF, a solvent in which aggregation of OPV and PERY compounds is generally not observed. Due to the strained geometry of **7**, the polarity of the solvent does not influence the formation of a face-to-face complex; therefore, the CT absorption is also observed in THF. As expected from the different reduction potentials (E_{red} = −1.02 and −0.80 V vs Fc/Fc^+ in CH_2Cl_2 for **2** and **3**, respectively),[15] the position of the CT absorption for unsubstituted perylene bisimide derivatives is already at considerably higher energies compared to the chlorine-substituted analogues.[40] Therefore, no attempt was made to monitor the CT absorption for **1**, because the CT state is even higher in energy as a result of the more negative reduction potential (E_{red} = −1.17 V) and because the ground-state absorption is considerably red-shifted due to the electron-donating character of the *tert*-butylphenoxy substituents. In addition, the bulkiness of this substituent can increase the distance between the OPV and PERY unit, thereby decreasing the intensity of the CT absorption band. As a result, the CT absorption is expected to be undetectable for the phenoxy-substituted OPV−PERY arrays, taking into account the spectral overlap and high molar absorption coefficient of the PERY-($S_1 \leftarrow S_0$) transition with respect to the CT transition.

Molecular Mechanics Calculations. Molecular mechanics (MM) calculations have been performed to gain a deeper insight into the packing of molecules **1**−**3**. We are mostly interested in assessing here, on a qualitative basis, the probability of H-type versus J-type aggregate formation among the three derivatives. To do so, we have considered a simple dimer model and followed the change in total energy as one molecule is slid with respect to the other. The geometry of the isolated chains was first optimized at the semiempirical Hartree−Fock Austin model 1 (AM1) level[41] while the OPV backbones were constrained to be fully planar and the long saturated chains attached to the terminal phenylene rings were replaced by methoxy groups. The results indicate that the perylene bisimide molecule is fully planar in **2** and distorted into a crosslike geometry in **1** and **3** (Figure 5). The AM1 calculations tend to position the phenoxy groups of **1** oriented along the *z*-direction above and below the perylene bisimide plane.[25] Since crystallographic data[24,42] indicate that such a conformation is unlikely in a densely packed assembly, we have considered in the following an extended

(38) Sadrai, M.; Bird, G. R.; Potenza, J. A.; Schugar, H. J. *Acta Crystallogr. C* **1990**, *C46*, 637−640.
(39) Van Herrikhuyzen, J.; Syamakumari, A.; Schenning, A. P. H. J.; Meijer, E. W. *J. Am. Chem. Soc.* **2004**, *126*, 10121−10127.
(40) For aggregates of **3**, the CT band is at 740 nm (1.68 eV), while the CT band in **7** is found at 640 nm (1.94 eV). In a first approximation, the difference in the energy of the CT bands (0.26 eV) scales with the difference between reduction potentials of the acceptor units (0.22 eV). This allows one to predict that the CT absorption in aggregates of **1** should be ∼0.15 eV above that of **7**, i.e., at ∼2.1 eV or 590 nm, which overlaps with the normal absorption of aggregate.
(41) Dewar, M. J. S.; Zoebisch, E. G.; Healy, E. F.; Stewart, J. J. P. *J. Am. Chem. Soc.* **1985**, *107*, 3902−3909.

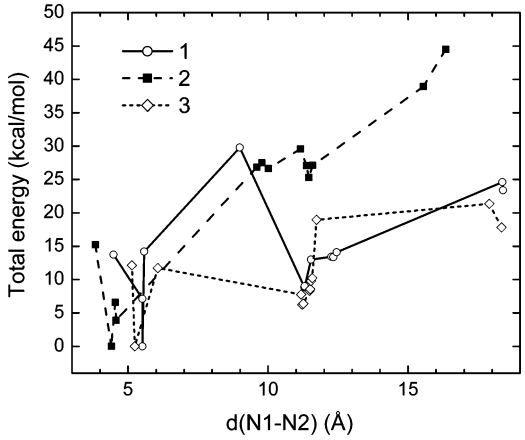

Figure 6. UFF-calculated evolution of the total energy of a dimer of **1**−**3** as a function of the degree of translation represented by the average distance [*d*(N1−N2)] between the perylene bisimide nitrogen atoms in the two interacting molecules. The energy of the global minimum is set equal to zero in all cases.

structure where the phenoxy groups are predominantly oriented along the *y*-axis to provide a more flat molecule (Figure 5).[43]

The potential energy curve has been generated using the UFF (universal force field) force field by calculating the energy of a stacked dimer, built from the isolated structure obtained at the AM1 level. The applicability of UFF to describe packing in molecular stacks has been validated in previous studies.[44] Nonbonding effects (van der Waals and Coulomb terms) in such long molecules have to be described with a long cutoff distance to provide a reliable stabilization energy upon packing. We have used the spline method with a spline-on and -off parameter set respectively to 200 and 300 Å; the convergence criterion for the optimization has been set at 10^{-5} kcal/mol, and the charges are computed by the default method. In our simulations, the stacking axis *z* is perpendicular to the perylene bisimide backbone in **2** and to its average molecular plane in **1** and **3**; the translation axis *x* is set parallel to the axis connecting the nitrogen atoms of the perylene bisimide moiety, as illustrated in Figure 5. Thirteen initial structures that differ by the magnitude of the translation along *x* were generated by positioning the two molecules at an intermolecular separation along *z* larger than the equilibrium distance (initial distances of 4.0 Å for molecule **2**, 5.0 Å for molecule **3**, and in the range 7−9 Å for molecule **1**). A full MM optimization is then achieved on the basis of these starting geometric configurations to yield optimized structures corresponding to local minima on the potential energy curve.

Figure 6 displays the total relative energy (with respect to the global minimum) versus translation along *x* (measured by the average distance between the perylene bisimide nitrogen atoms in the two interacting molecules), as calculated at the UFF level for the three molecules. The absolute energies and shifts are collected in Table 1 provided in the Supporting Information. Analysis of the results shows the following.

(i) The fully cofacial geometry (zero displacement along *x*) does not correspond to a stable configuration in any of the three compounds. This is mostly due to steric effects between the substituents in **1**, Coulomb repulsion between the negatively charged nitrogen atoms in **2**, and Coulomb repulsion between the chlorine atoms in **3**. The latter effect leads to the largest intermolecular spacing for **3** (5.14 Å) compared to **1** (4.48 Å) and **2** (3.83 Å). The global minimum is obtained for a slightly displaced H-type configuration, corresponding to a shift along *x* of ∼4.2 Å in **1**, ∼2.8 Å in **2**, and ∼4.2 Å in **3**.

(ii) A local minimum is observed for the three compounds with displacements along the *x* direction of around 12 Å, which corresponds to a J-like architecture (the distance between the two nitrogen atoms of a perylene bisimide molecule is indeed ∼11.3 Å). However, this structure is found to be significantly more stable in **1** and **3** with respect to **2**. This can be rationalized by the fact that the steric effects that destabilize the H-type aggregate in **1** and **3** are progressively switched off when sliding the two molecules on top of one another, thereby allowing for bonding van der Waals interactions. As similar steric effects are absent in **2**, a monotonic decrease of the interaction energy as a function of translation along *x* is predicted in that case. We also stress that the relative stability of J-like vs H-like architectures is underestimated in our dimer calculations, due to the smaller interaction surface. We expect that upon building a 3D model for the packing of **1** and **3**, J-aggregates will be further favored. The calculations are thus consistent with the experimental data pointing to the fact that H-aggregates are observed only for **2**, while for **1** and **3**, steric repulsion between the substituted perylene bisimide cores drives the structures toward a J-type arrangement.

Photoinduced Charge Separation and Recombination. The dynamics of the photoinduced charge separation in MCH has been studied by transient photoinduced absorption spectroscopy (Figure 7), by monitoring the characteristic transient absorption of the $OPV^{+\bullet}$ radical cation at 1450 nm,[13] after excitation at 455 nm. These measurements reveal remarkable differences in the charge transfer kinetics for the aggregated state when compared to the same compounds in the molecularly dissolved state in *o*-dichlorobenzene (ODCB, $\epsilon = 9.93$) and toluene ($\epsilon = 2.38$), despite the fact that the polarity of the latter is similar to that of MCH ($\epsilon = 2.02$). In a first approximation, the rate for charge separation is expected to be the lowest in MCH, because the driving force ($-\Delta G_{CS}$) decreases in less polar solvents (eqs 1 and 2).[45,46]

$$-\Delta G_{CS} = E(S_1) - G_{CS} \quad (1)$$

$$G_{CS} = e[E_{ox}(D) - E_{red}(A)] - \frac{e^2}{4\pi\epsilon_0\epsilon_s R_{cc}} - \frac{e^2}{8\pi\epsilon_0}\left(\frac{1}{r^+} + \frac{1}{r^-}\right)\left(\frac{1}{\epsilon_{ref}} - \frac{1}{\epsilon_s}\right) \quad (2)$$

Actually, an estimate of the energy of the intramolecular charge-separated state by means of eqs 1 and 2 indicates that for **1** this state is degenerate with the first singlet-excited state of the perylene bisimide moiety ($\Delta G_{CS} = 0.00$ eV). Because

(42) Osswald, P.; Leusser, D.; Stalke, D.; Würthner, F. *Angew. Chem., Int. Ed.* **2005**, *44*, 250−253.
(43) Würthner, F. *Chem. Commun.* **2004**, 1564−1579.
(44) Leclère, Ph.; Hennebicq, E.; Calderone, A.; Brocorens, P.; Grimsdale, A. C.; Müllen, K.; Brédas, J. L.; Lazzaroni, R. *Prog. Polym. Sci.* **2003**, *28*, 55−81.
(45) Weller, A. *Z. Phys. Chem.* **1982**, *133*, 93−8.
(46) In this equations $E_{ox}(D)$ and $E_{red}(A)$ are the oxidation and reduction potentials of the donor and acceptor molecules or moieties measured in a solvent with relative permittivity ϵ_{ref}; $E(S_1)$ is the energy of the excited state from which the electron transfer occurs and R_{cc} is the center-to-center distance of the positive and negative charges in the charge-separated state. The radii of the positive and negative ions are given by r^+ and r^-, ϵ_s is the relative permittivity of the solvent, $-e$ is the electron charge, and ϵ_0 is the vacuum permittivity.

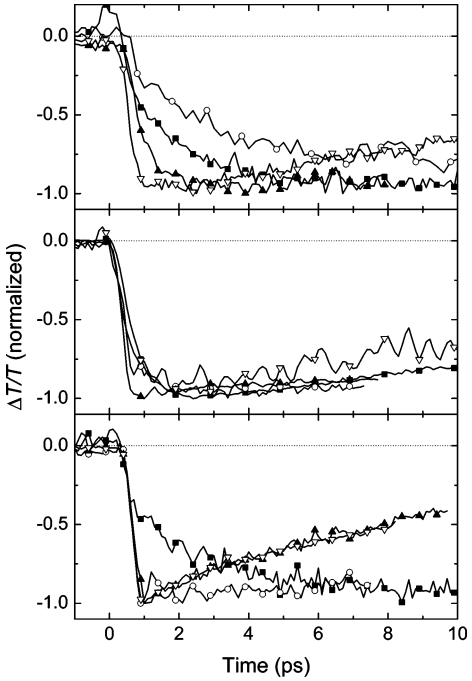

Figure 7. Transient photoinduced absorption dynamics probing charge separation of 5×10^{-5} M solutions of **1** (top), **2** (middle), and **3** (bottom) at room temperature in ODCB (solid squares), toluene (open circles), MCH (solid triangles) and in the solid state (open triangles). For all measurements an excitation wavelength of 455 nm was used with detection of the $OPV^{+\bullet}$ absorption at 1450 nm. The experimentally obtained values for $\Delta T/T$ at the maximum intensity of the transient PIA trace range from 2×10^{-3} to 10^{-2} for the various experiments.

the driving force for the charge separation reaction for **1** is considerably smaller than the reorganization energy,[15] the charge transfer occurs in the normal Marcus region, and hence, the rate constant (k_{CS}) increases with increasing driving force.[47] Therefore, if charge separation is present at all, the rate for charge separation for compound **1** in a molecularly dissolved state in MCH is expected to be slow. In contrast with these expectations, the charge separation reaction for **1** in MCH occurs at a considerably higher rate ($k_{CS} = 1.2 \times 10^{12}$ s^{-1}) than in ODCB ($k_{CS} = 4.6 \times 10^{11}$ s^{-1}) or in toluene ($k_{CS} = 2.7 \times 10^{11}$ s^{-1}). This difference can only be rationalized by the presence of aggregated species in MCH.

For **2** and **3**, the photoinduced charge separation in MCH is equally fast and occurs with rate constants of $k_{CS} = 2.2 \times 10^{12}$ and 2.9×10^{12} s^{-1}, respectively.[48] We previously established that for **2** and **3**, the forward charge transfer occurs close to the Marcus optimal region.[15] Under these conditions, it is difficult to predict how k_{CS} changes with solvent polarity, and hence, the high rate constants cannot directly be associated with the aggregated nature of the compounds.

To explain the fast forward electron-transfer reaction in **1** in MCH, we note that the formation of J-type aggregates enables charge separation to occur via an intermolecular process rather than intramolecularly, because the intermolecular distance between the OPV and PERY moieties is shorter than the intramolecular distance (Figure 3). This implies that the distance of 14 Å between the OPV and PERY chromophores[15] used for the calculation of the driving force is not applicable for **1** when it is in a J-type aggregate. A molecular mechanics calculation of **7** revealed two nonperfectly parallel OPV and PERY chromophores at a distance of about 4 Å. On the basis of this result, we estimate the intermolecular distance of molecules in the π-stacked systems **1**−**3** to be ∼4 Å. This short distance introduces a considerable increase in the driving force for charge separation in MCH compared to calculations assuming a 14 Å distance (Figure 8). For **1**, the driving force, calculated from eq 1, increases from ∼0 eV at 14 Å to −1.27 eV at a distance of 4 Å. Interestingly, the driving force for charge separation in MCH for distances around 4 Å is higher than in ODCB ($\Delta G_{CS} = -0.76$ eV) and in toluene ($\Delta G_{CS} = -0.14$ eV) at 14 Å, consistent with the observed decreasing rate constant for charge separation for **1** going from MCH to ODCB, and toluene.

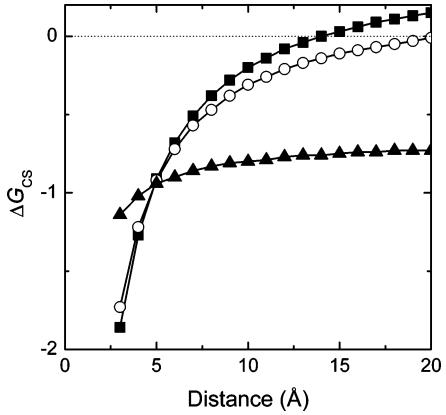

Figure 8. Calculated driving force for charge separation (ΔG_{CS}) for **1** at various interchromophoric distances in MCH (squares), toluene (circles), and ODCB (triangles).

We note that this simple analysis ignores any changes in electronic coupling when going from an intramolecular to an intermolecular charge separation process. In these molecules, the intramolecular coupling is fairly weak (see ref 15, 6 meV) due to the nodal plane in the frontier orbitals of the perylene bisimide core.[14,43] For compound **7**, the electronic coupling for the face-to-face charge transfer has been calculated to be 8−9 meV when the electron-transfer originates from the lowest singlet state in the diad ($PERY(S_1)$).[14] These numbers suggest that the electronic coupling is similar for the two processes, but we caution that for intermolecular processes the electronic coupling can vary strongly with the mutual orientation of the molecules.[49]

Of course it is of interest to study if the changes in the rates for charge recombination (k_{CR}) between the molecularly dissolved and aggregated states can also be rationalized by considering the shortest OPV−PERY distances as for charge separation. When the driving force for charge separation increases as a result of the shorter distance between the two chromophores, the driving force for charge recombination ($-\Delta G_{CR}$) will diminish to satisfy that $E(S_1) = -(\Delta G_{CS} + \Delta G_{CR})$. Accordingly, Figure 9 shows that the driving force for charge recombination will increase for longer donor−acceptor distances. For the J-type aggregates of **1** in MCH, the driving force for intermolecular charge recombination at 4 Å of ΔG_{CR}

(47) Marcus, R. A. *Rev. Mod. Phys.* **1993**, *65*, 599−610.
(48) It should be noted here that differences in rate constants for the charge separation and recombination rates between the three studied compounds in the same solvent cannot be directly related to the supramolecular structure. The observed differences originate from the different acceptor strength induced by the substituents on the bay position of the perylene bisimide moiety.
(49) Lemaur, V.; Steel, M.; Beljonne, D.; Brédas, J.-L.; Cornil, J. *J. Am. Chem. Soc.* **2005**, *127*, 6077−6086.

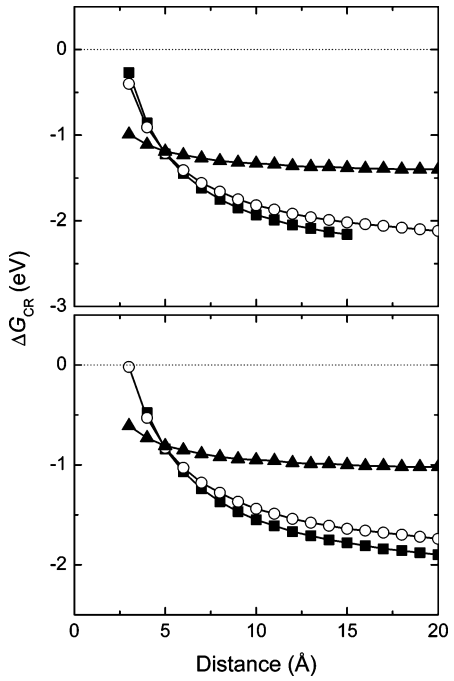

Figure 9. Calculated driving force for charge recombination (ΔG_{CR}) in **1** (top) and **3** (bottom) for different interchromophoric distances in MCH (squares), toluene (circles), and ODCB (triangles).

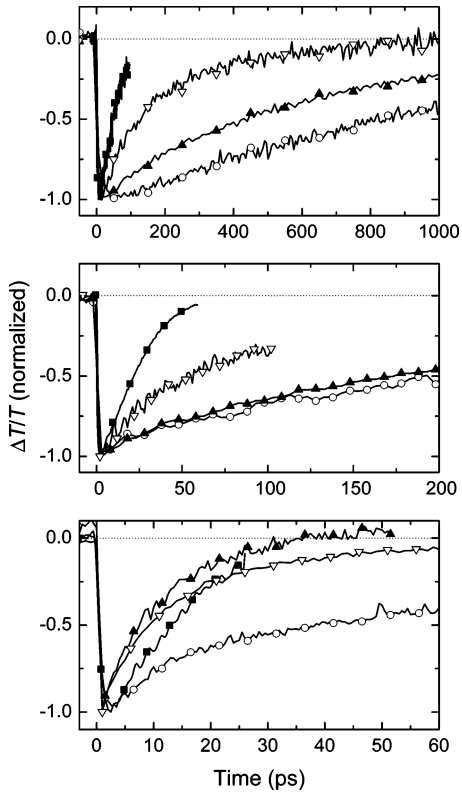

Figure 10. Transient photoinduced absorption dynamics probing charge recombination of 5×10^{-5} M solutions of **1** (top), **2** (middle), and **3** (bottom) at room temperature in ODCB (solid squares), toluene (open circles), MCH (solid triangles), and the solid state (open triangles). For all measurements an excitation wavelength of 455 nm is used, with detection of the $OPV^{+\bullet}$ absorption at 1450 nm. The experimentally obtained values for $\Delta T/T$ at the maximum intensity of the transient PIA trace range from 2×10^{-3} to 10^{-2} for the various experiments.

$= -0.86$ eV is therefore less than the value of -1.99 eV for intramolecular recombination in toluene at 14 Å.

Charge recombination in arrays **1**−**3** is in the Marcus inverted region,[15] and as a consequence the decrease in $-\Delta G_{CR}$ leads to a faster charge recombination (i.e., a shorter lifetime of the charge-separated state). In agreement with this prediction, we find experimentally that the rate for charge recombination for **1** in MCH ($k_{CR} = 2 \times 10^9$ s^{-1}) (Figure 10) is higher than in toluene ($k_{CR} < 8 \times 10^8$ s^{-1}). We note that the photoinduced absorption of **1** in MCH at elevated temperatures, where this compound is in its molecularly dissolved state, leads to the same kinetics as that observed in toluene at room temperature.[12] This demonstrates that the arrangement of the supramolecular structure in the aggregated state causes the higher recombination rate.

For **3**, the donor−acceptor distance would be similarly reduced from 14 Å to about 4 Å when it forms J-type aggregates, and as a consequence, charge recombination should be faster in the aggregated state than in a molecularly dissolved state when solvents of similar polarity are used. The rate of charge recombination observed experimentally in MCH ($k_{CR} = 8.3 \times 10^{10}$ s^{-1}) is indeed considerably higher than the rate measured in toluene ($k_{CR} = 1.6 \times 10^{10}$ s^{-1}) and even slightly higher than in ODCB ($k_{CR} = 7.9 \times 10^{10}$ s^{-1}). This is in full agreement with the lower energy of the charge-separated state for **3** as a result of its intermolecular nature and parallels the results obtained for **1**. Moreover, the rate found for **3** in MCH is identical to the rate obtained for thin films of the same molecule. This suggests that in the solid state the donor and acceptor moieties also pack in a face-to-face configuration, similar to the J-type structure; this is further confirmed by the nearly identical UV−vis absorption in the film and in the aggregates. This is in accordance with the proposed morphologies for other OPV−PERY systems[14] and is a frequently observed packing motif for covalent donor−acceptor polymers.[50−53]

The formation of the complex of **4** and **5** implies that the donor and acceptor molecules are in very close proximity and therefore a photoinduced charge separation can be expected. The transient photoinduced absorption time trace of a 1:1 mixture of **4** and **5** recorded after exciting the sample at 455 nm and detecting at the $OPV^{+\bullet}$ absorption at 1450 nm confirms the intermolecular electron transfer between **4** and **5** in the mixed aggregate (Figure 11). The rapid rising of the signal (<1 ps) indicates that charge separation occurs at a much faster rate than expected for a diffusion-limited reaction between two molecularly dissolved molecules. Strikingly, the transients for **3** and the mixture of **4** and **5** are identical. Since the molecules **4** and **5** stack in a sandwich-type structure, we imagine that this geometry is most likely also present for **3**, in full agreement with the previous observations. This indicates that the CT and $\pi-\pi$ interactions between the OPV and PERY moieties determine to a large extent the structure of the complex in the solid state and in the aggregate.

Charge separation in **2** is equally fast in all solvents and not strongly affected by polarity or aggregation (Figure 7) and, hence, differs strongly from the behaviors of **1** and **3**. Charge recombination in **2**, however, varies more strongly and is faster in ODCB (Figure 10). In strong contrast with the results for **1** and **3**, the rate for charge recombination of **2** dissolved in toluene

(50) Lokey, R. S.; Iverson, B. L. *Nature* **1995**, *375*, 303−305.
(51) Nguyen, J. Q.; Iverson, B. L. *J. Am. Chem. Soc.* **1999**, *121*, 2639−2640.
(52) Zych, A. J.; Iverson, B. L. *J. Am. Chem. Soc.* **2000**, *122*, 8898−8909.
(53) Ghosh, S.; Ramakrishnan, S. *Macromolecules* **2005**, *38*, 676−686.

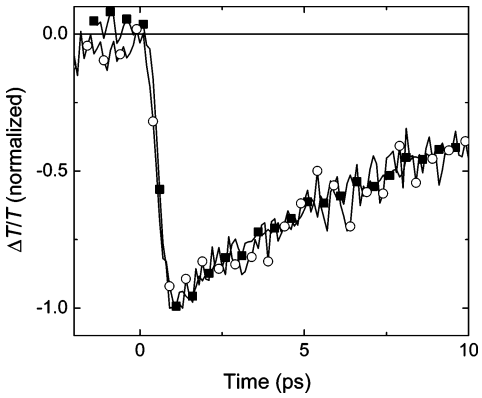

Figure 11. Transient photoinduced absorption dynamics in MCH of **3** (solid squares, 5×10^{-5} M) and a 1:1 mixture of compounds **4** and **5** (open circles, 10^{-4} M). For both measurements an excitation wavelength of 455 nm is used, with detection of the $OPV^{+\bullet}$ absorption at 1450 nm. The experimentally obtained values for $\Delta T/T$ at the maximum intensity of the transient PIA trace are 3×10^{-3} and 10^{-3}, respectively, for compound **3** and the mixture of **4** and **5**.

or as aggregates in MCH are identical ($k_{CR} = 3.0 \times 10^9$ s^{-1}). Apparently, the intermolecular effects that arise when **2** forms aggregates do not enhance the recombination rate, in contrast to the results observed for **1** and **3**. This is in full agreement with the proposed molecular picture of an H-type aggregate, where the intramolecular distance between the OPV and PERY moieties remains the shortest distance between the chromophores. At the same time we conclude that delocalization of positive or negative charges in the H-type aggregates along a stack of chromophores does not enhance the lifetime or does not occur. In agreement with recent work by Wasielewski et al.,[54] we therefore conclude that in aggregates of donor–acceptor compounds where the donors stack on donors and the acceptors on acceptors (H-type), the influence of aggregation is small and the photophysical properties of the aggregate resemble that of the molecular dissolved state.

Conclusions

The supramolecular structures of aggregates of three different OPV–PERY–OPV arrays **1**–**3** in MCH have been characterized in terms of H- and J-type aggregates using absorption spectroscopy and molecular mechanics calculations. In these aggregates, highly efficient and fast photoinduced charge separation occurs. For the H-type aggregates of **2**, only minor differences are found for the kinetics of charge separation and recombination when the aggregates are compared to a nonaggregated, molecularly dissolved state in an apolar solvent. In contrast, the forward and backward electron transfer rates are considerably faster in J-type aggregates (**1** and **3**) than in solution, even for a polar solvent. These results can consistently be rationalized by considering the new close contacts of OPV and PERY chromophores that are created in J-type aggregates but are absent in H-type aggregates of the OPV–PERY–OPV arrays. For the bay-substituted derivatives **1** and **3**, which are twisted in the middle of the PERY chromophore, a shift in the direction of the long axis of the molecule is triggered by steric effects and is fully supported by the spectroscopic data. The shortest donor–acceptor distance is identified as the most important parameter in accelerating charge-transfer reactions, both separation and recombination, under conditions of J-type aggregation in an apolar medium. Ultimately, supramolecular interactions such as hydrogen bonding, charge-transfer interactions, and $\pi-\pi$ stacking of functional π-conjugated systems[34,43,55,56] may be used to create artificial systems with predefined photophysical properties that convert, store, or use photon energy. The results presented here demonstrate that a balance between molecular properties and intermolecular interactions is crucial to the photophysics of self-assembled architectures of functional molecules and that distance is a simple, but very important, parameter.

Experimental Section

UV/visible/near-IR absorption and fluorescence spectra were recorded on a Perkin-Elmer Lambda 900 and an Edinburgh Instruments FS920, respectively. Circular dichroism measurements were performed on a Jasco J-600 spectropolarimeter. The solvents MCH, toluene, and ODCB were of spectroscopic grade and used as received. The synthesis of compounds **1**,[12] **2**,[13] **3**,[15] **4**,[57] **5**,[25] **6**,[58] and **7**[14] has been published elsewhere. Detailed information on the parameters used for the calculation of the driving force for charge separation and recombination can be found in ref 15. All experiments are performed at room temperature unless stated otherwise.

The femtosecond laser system used for pump–probe experiments consisted of an amplified Ti/sapphire laser. The single pulses from a cw mode-locked Ti/sapphire laser were amplified by a Nd:YLF laser using chirped pulse amplification, providing 150 fs pulses at 800 nm with an energy of 750 μJ and a repetition rate of 1 kHz. The pump pulses at 455 nm were created via optical parametric amplification (OPA) of the 800 nm pulse by a BBO crystal into infrared pulses that were then two times frequency doubled via BBO crystals. The probe beam was generated in a separate optical parametric amplification setup in which the 1450-nm pulses were created and a RG 850-nm cutoff filter was used to avoid contributions of residual probe light (800 nm) from the OPA. The pump beam was focused to a spot size of about 1 mm^2 with an excitation flux of 1 mJ cm^{-2} per pulse. The probe beam was reduced in intensity compared to the pump beam by using neutral density filters. The pump beam was linearly polarized at the magic angle of 54.7° with respect to the probe, to cancel out orientation effects in the measured dynamics. The temporal evolution of the differential transmission was recorded using an InGaAs detector by a standard lock-in technique at 500 Hz. All samples were measured in cells with a path length of 1 mm.

Acknowledgment. This work has been supported by CW-NWO in the PIONIER program, the DFG (grant Wu 317/5), and the European Integrated project NAIMO (NMP4-CT-2004-500355). The research of S.M. has been made possible by a fellowship of the Royal Dutch Academy of Arts and Sciences. J.C. and D.B. are research fellows of the Belgian National Fund for Scientific Research (FNRS).

Supporting Information Available: Table with the UFF energies of the dimers as a function of the degree of translation. Experimental data on the circular dichroism spectra of **1**–**3** in MCH. This material is available free of charge via the Internet at http://pubs.acs.org.

JA0568042

(54) Rybtchinski, B.; Sinks, L. E.; Wasielewski, M. R. *J. Phys. Chem. A* **2004**, *108*, 7497–7505.
(55) Piotrowiak, P. *Chem. Soc. Rev.* **1999**, *28*, 143–150.
(56) Schenning, A. P. H. J.; Jonkheijm, P.; Peeters, E.; Meijer, E. W. *J. Am. Chem. Soc.* **2001**, *123*, 409–416.
(57) Peeters, E.; Ramos, A. M.; Meskers, S. C. J.; Janssen, R. A. J. *J. Chem. Phys.* **2000**, *112*, 9445–9454.
(58) Demmig, S.; Langhals, H. *Chem. Ber.* **1988**, *121*, 225–230.